https://doi.org/10.3311/PPch.41026

Periodica Polytechnica Chemical Engineering, 69(4), pp. 649–661, 2025

Effect of Graphene Oxide on the Mechanical, Thermal, and Fire-retardant Properties of Carbon Fiber Reinforced Epoxy Composites

Sekar Azhagarsamy[1], Narayanan Pannirselvam[1*]

[1] Department of Civil Engineering, College of Engineering and Technology, SRM Institute of Science and Technology, 603 203 Kattankulathur, Tamilnadu, India
[*] Corresponding author, e-mail: pannirsn@srmist.edu.in

Received: 15 May 2025, Accepted: 04 September 2025, Published online: 23 September 2025

Abstract

The utilization of carbon fiber reinforced polymer (CFRP) composites has garnered considerable interest due to their lightweight characteristics, exceptional strength, and improved chemical resistance. This study examines CFRP composite's mechanical and thermal performance, emphasizing the influence of epoxy resin and graphene oxide (GO) on improving structural qualities. CFRP is extensively utilized in aerospace, automotive, and civil engineering sectors, especially for structural reinforcement and restoration. This study investigates the impact of GO ranging from 0, 0.05, 0.1, 0.3, and 0.5 wt.% on CFRP laminates mechanical characteristics produced *via* the hand layup technique with bidirectional plies. Mechanical testing, performed by ASTM standards, demonstrated that including GO enhanced composite density, tensile strength, and flexural strength owing to improved interfacial bonding. Fourier-transform infrared spectroscopy confirmed strong chemical interactions through characteristic peaks of carbonyl and ether groups. Thermogravimetric analysis and differential scanning calorimetry revealed enhanced thermal stability and increased glass transition temperatures from 102.31 °C for neat CFRP to 163.16 °C at 0.3 wt.% GO. Furthermore, GO demonstrated fire-retardant characteristics, markedly decreasing self-extinguishing duration by 33% and combustion rate. At 0.3 wt.% GO tensile strength increased by 24.5%, flexural strength by 21.3%, and impact strength by 18.7% compared to neat CFRP. The findings indicate that CFRP laminates reinforced with 0.3 wt.% GO content exhibit enhanced mechanical performance and fire resistance, rendering them appropriate for advanced structural applications in civil engineering and other fields.

Keywords

CFRP laminates, epoxy resin, graphene oxide, mechanical properties, thermal properties

1 Introduction

Fiber reinforced polymer (FRP) composites have garnered significant interest in the construction and structural industries due to their exceptional strength-to-weight ratio, corrosion resistance, and durability [1]. Among various FRP types, the carbon fiber reinforced polymer (CFRP) is widely recognized for its outstanding tensile strength, rigidity, and fatigue resistance [2, 3]. These characteristics make CFRP composites ideal for applications requiring superior mechanical performance and long-term durability [4]. CFRP's exceptional tensile strength, rigidity, and fatigue resistance renders it an optimal selection for applications demanding superior mechanical performance and durability. Despite these advantages, CFRP systems often face limitations due to interfacial bonding issues between the carbon fibers and the epoxy matrix, which can hinder load transfer efficiency and structural performance [5, 6]. Researchers have concentrated on enhancing the bonding characteristics of CFRP composites by altering the epoxy resin matrix to address these constraints [7, 8]. A promising method to improve the mechanical and interfacial properties of CFRP composites is the integration of nanofillers into the resin matrix. Nanomaterials, especially graphene-based additives, exhibit significant potential in overcoming the adhesion and strength constraints of CFRP composites [9–11]. Graphene nanofillers, including graphene oxide (GO) and graphene nanoplatelets (GnPs), have arisen as superior reinforcements in polymer matrices owing to their exceptional mechanical and thermal characteristics [12]. GO possesses an extraordinarily high Young's modulus (~1 TPa), fracture strength (~130 GPa),

Cite this article as: Azhagarsamy, S., Pannirselvam, N. "Effect of Graphene Oxide on the Mechanical, Thermal, and Fire-retardant Properties of Carbon Fiber Reinforced Epoxy Composites", Periodica Polytechnica Chemical Engineering, 69(4), pp. 649–661, 2025. https://doi.org/10.3311/PPch.41026

and thermal conductivity (~5300 W/m×K), rendering it an outstanding contender for the enhancement of CFRP composites [13, 14]. The integration of GO into the CFRP epoxy matrix significantly improves tensile and flexural strength by promoting superior load transmission between the carbon fibers and the polymer. Moreover, GO improves interfacial adhesion, diminishes micro-void formation, and elevates thermal stability [15]. It functions as a flame retardant by creating a protective char layer that inhibits ignition and reduces heat release rates, enhancing CFRP laminates' fire resistance.

Notwithstanding these benefits, the efficacy of GO-enhanced CFRP composites is significantly contingent upon the quality of GO dispersion [16]. Inadequate dispersion may result in agglomeration, increased resin viscosity, and processing difficulties, which can adversely impact mechanical performance. Consequently, attaining uniform dispersion and optimizing GO concentration is essential in enhancing GO-modified CFRP composites. [17, 18].

1.1 GO-enhanced CFRP composites

GO is a minuscule particle, generally measuring between 1 and 100 nm, incorporated into diverse materials to improve their characteristics. These particles are extensively utilized in composite materials, polymers, coatings, and various substances to enhance mechanical, thermal, electrical, or optical properties [19]. GO, due to their high surface area-to-volume ratio, can substantially modify material properties even at minimal concentrations, rendering them optimal for customizing materials for specific applications, including the fabrication of lightweight yet robust composites, the production of conductive polymers or the enhancement of barrier coatings [20]. GO is integrated into the polymer matrix of CFRP laminates during production, where they are uniformly scattered inside the resin. This incorporation provides advantages such as superior mechanical qualities, excellent thermal stability, elevated electrical conductivity, and reduced mass. GO is distinguished among GO by its unique structure, a monolayer of carbon atoms organized in a two-dimensional honeycomb lattice, and excellent qualities, including outstanding mechanical strength, high thermal and electrical conductivity, and an extensive surface area [21, 22]. This work utilized GO with an average flake thickness of 12 nm, a particle size of 4500 nm, and a specific surface area of 80 m^2/g, illustrating its capacity to enhance the performance of CFRP composites markedly. The morphology of the GO used in this study is shown in Fig. 1.

This research reveals significant insights into the capabilities of GO-modified CFRP composites for high-performance structural applications, especially in civil infrastructure that demands improved strength, durability, and fire resistance.

Fig. 1 Graphene oxide (GO)

2 Materials and methodology

2.1 Components utilized in CFRP composites

The research employed bidirectional CFRP woven fabric, weighing 200 g/m^2 with fiber diameters ranging from 6–8 μm, which was procured from Fiber Region Pvt. Ltd., Chennai, India. GO was obtained from Nano Research Lab Pvt. Ltd., India. Table 1 outlines the properties of the CFRP and GO reinforcing materials. Following the supplier's instructions, the matrix was created with Araldite Klear 4 Plus epoxy resin and a specified hardener. For optimal adhesion, the epoxy resin and hardener were combined in a ratio of 10 parts resin to 8 parts hardener.

2.2 The manufacturing process of CFRP composites

Fig. 2 depicts the CFRP composite laminate production process utilizing a static compression approach, employing either hand or wet layup methods. The procedure commenced with

Table 1 Properties of CFRP and GO

Material	Property	Value
CFRP	Yield strength (MPa)	1720–3600
	Density (g/cm^3)	1.55–1.76
	Ultimate tensile strength (MPa)	1755–3690
	Tensile modulus (GPa)	120–580
	Elongation (%)	3.0–10
	Thickness (nm)	0.8–2
GO	Color	Black-grey powder
	Number of layers	1–3
	Purity (%)	99.5
	Density (g/cm^3)	2.3
	Melting point range (°C)	3697

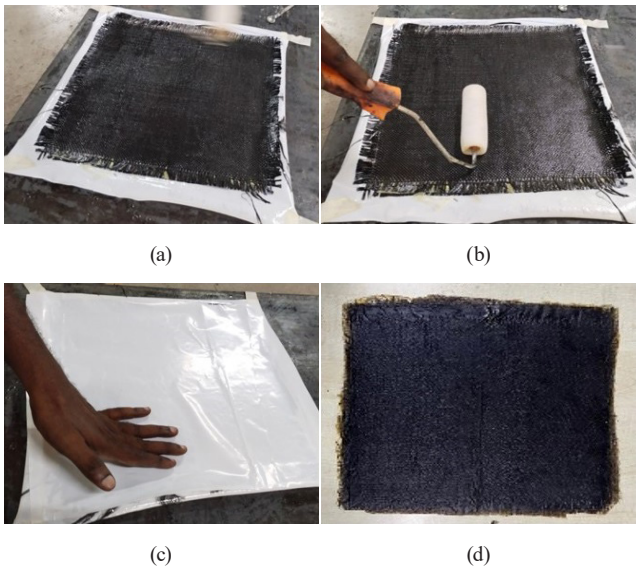

Fig. 2 (a) Releasing fume with CFRP; (b) CFRP with resin coating; (c) Drying process of laminate; (d) Lamination mat after compression

the formulation of the GO-infused resin. GO were incorporated into the resin at room temperature utilizing a magnetic stirrer. The mixture was agitated at 250 rpm for 30 min to ensure complete homogeneity. The hardener was initially incorporated into the GO-resin blend at a 1:10 ratio and agitated at 300 rpm to achieve a homogeneous, well-dispersed mixture. The wet layup procedure involved applying prepared GO-enhanced resin to the fibers in the mold using a brush and roller at ambient temperature. Spacers were inserted between the mold plates to guarantee consistent thickness throughout the laminate. Following a preliminary 1 h curing phase under light pressure, the laminates were permitted to cure at ambient temperature for 48 h.

2.3 Tensile test

The laminate samples that were going to be used for the tension test (AGX-V50 kN Universal Testing Machine, Shimadzu) were prepared using a water jet to cut them with precision, as depicted in Fig. 3. The dimensions of the samples were 165 × 20 × 2.98 mm. The tensile tests were carried out at a 2 mm/min loading speed, per the ASTM D638-14 standard [23] requirement for quasistatic testing, which has a strain rate of 5% per min. This technique was implemented to guarantee precise and uniform data collection. Key variables, including strain, tensile stress, ultimate tensile strength, and break load, were measured during the testing process to assess the performance of the material.

2.4 Flexure test

The flexural test was performed to ascertain the bending modulus of the CFRP laminate, measuring its resistance to deformation under bending forces. Specimens were

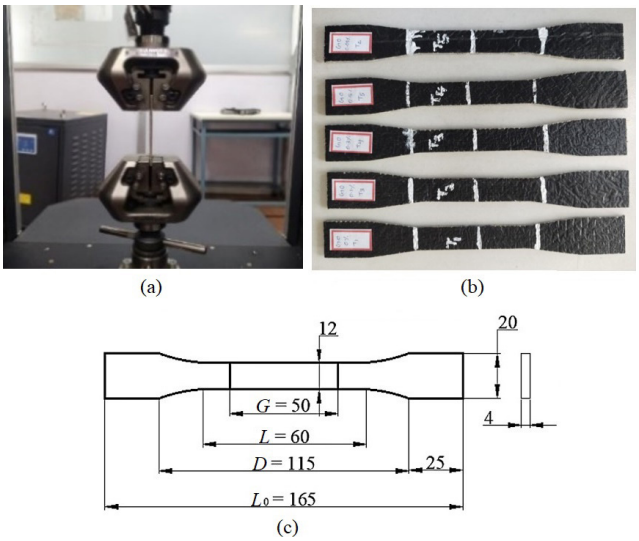

Fig. 3 (a) Tension test setup; (b) Tensile coupon samples; (c) Dimensions of tensile coupon testing (all dimensions are in mm)

prepared and evaluated utilizing a three-point bending apparatus by ASTM D790-17 standard [24] criteria. The testing apparatus had a press and supports with a diameter of 20 mm, and the loading rate was sustained at 0.5 mm/min (TUE-CN 200 kN Universal Testing Machine, FSA Pvt. Ltd.). During the examination, specimens were placed on two support pins separated by a distance of D, while a central force F was exerted through a single loading pin. The force-displacement approach (Eq. (1)) was utilized to get the flexural modulus E, using the equation that includes m (initial slope of the load-deflection curve), h (laminate thickness), b (specimen width), and L (span length). The test was performed at a 2 mm/min speed to maintain consistency and reliability, as depicted in Fig. 4.

$$E = \frac{mL^3}{4bh^3} \tag{1}$$

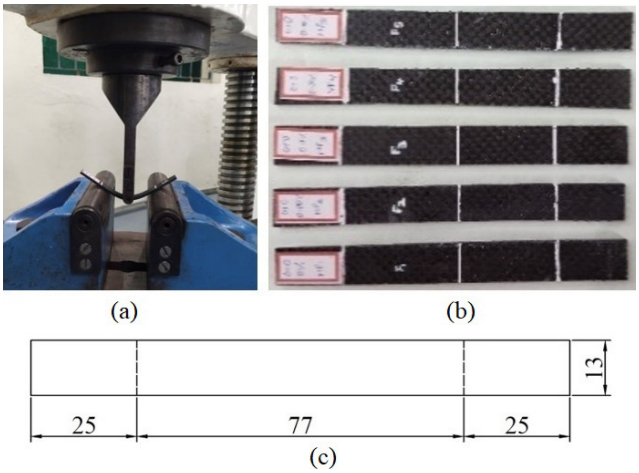

Fig. 4 (a) The flexural test setup; (b) Flexural test samples; (c) Dimensions of flexural testing (all dimensions are in mm)

2.5 Impact test

The impact strength of the produced CFRP composite laminates was assessed using the Charpy impact test by ASTM D256-24 standard [25] (Charpy impact tester, Tinius Olsen). In this experiment, a pendulum, launched at a 135-degree angle, impacts the specimen with a regulated force to produce a fracture. The energy absorbed during fracture was documented to evaluate the material's impact resistance. Specimens were fabricated to conventional dimensions to guarantee uniformity, as depicted in Fig. 5.

2.6 Water absorption test

CFRP composites are synthetic materials recognized for their superior strength-to-weight ratio and resistance to environmental influences compared to natural fiber composites. Despite their synthetic composition, CFRP composites can absorb moisture when subjected to humid conditions or submerged in water. This moisture absorption may arise from the hydrophilic characteristics of the polymer matrix and possible micro-voids or defects at the fiber-matrix interface. Ultimately, this may result in a deterioration of mechanical and service attributes. Consequently, it is essential to examine the water absorption characteristics of CFRP composites to assess their efficacy in moisture-laden environments. The specimens were prepared for the water absorption test according to the ASTM D570-22 standard [26]. The CFRP specimens were immersed in distilled water at room temperature for 7 days. The samples were systematically extracted from the water at consistent intervals, and their surfaces were meticulously dried with a cloth to eliminate excess moisture before weighing. The proportion of water absorption in the composites was calculated using Eq. (2):

$$W = \frac{W_t - W_i}{W_i} \times 100, \tag{2}$$

where W_t represents the specimen's final mass after exposure to water, and W_i is the initial mass of the specimen before exposure.

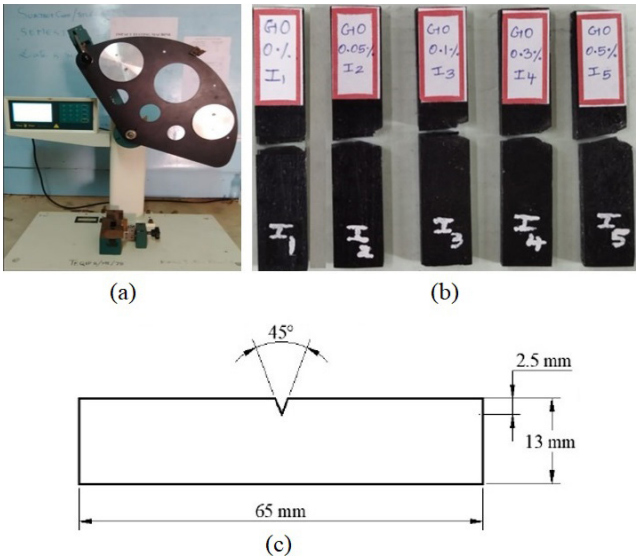

Fig. 5 (a) The impact test setup; (b) Impact test samples; (c) Dimensions of impact testing

2.7 Flammability tests

A flammability test was conducted to analyze the combustion characteristics of CFRP composites using GO, as illustrated in Fig. 6. Test specimens were prepared for flame testing in both vertical and horizontal orientations. The vertical flame test sample length was 125 mm, while its breadth measured 13 mm. The sample was positioned vertically during this experiment and subjected to a 10 s ignition at its lower extremity. The flammability of the specimen was assessed

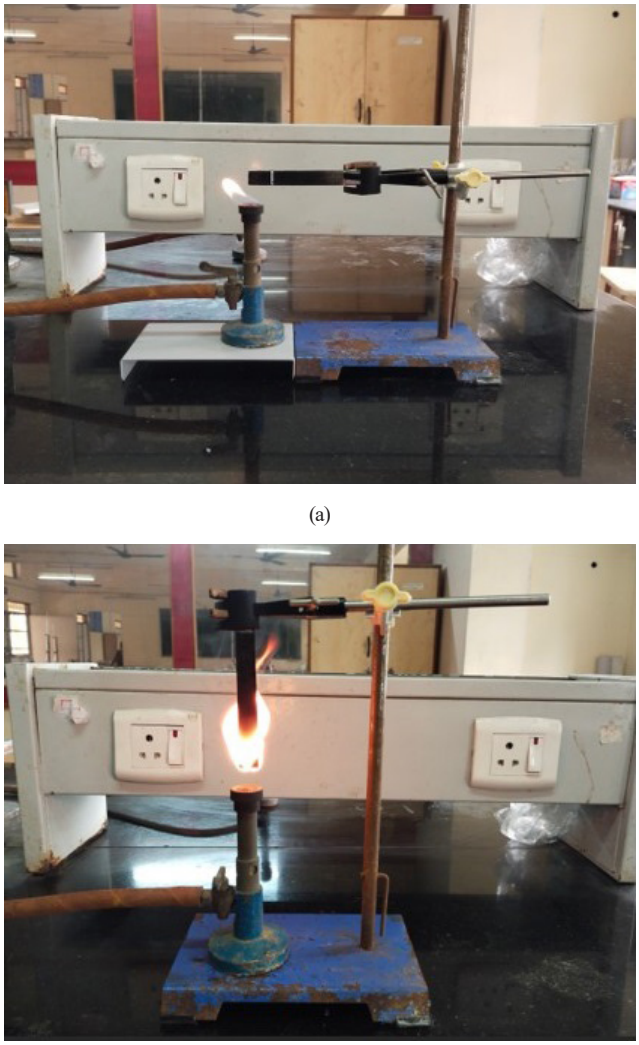

Fig. 6 (a) Horizontal flame testing; (b) Vertical flame testing

by measuring the time of self-extinguishment. The specimen was securely positioned horizontally for this test and evaluated at distances of 25 mm and 100 mm. The unconnected segment of the sample was ignited for 30 sec, and the rate at which the composite burned was determined.

2.8 X-ray diffraction (XRD)

XRD research was conducted to investigate the crystalline properties of the GO integrated into the CFRP/epoxy composite. A monochromatic CuKα radiation source (λ = 0.1542 nm) operated at 40 kV and 30 mA was utilized (X-Ray Diffractometer (XRD), BRUKER USA D8 Advance, Davinci). The diffraction pattern was documented in a 2θ range of 0° to 100° with a step increment of 0.05°. The acquired XRD peaks were examined to verify the existence of GO, evaluate its dispersion, and identify any structural alterations resulting from interaction with the epoxy matrix.

2.9 Morphology and fractography

The surface morphology and fracture properties of the GO-reinforced CFRP/epoxy composite were examined using a high-resolution scanning electron microscope (HR-SEM). The investigation aimed to assess the dispersion of GO, fiber-matrix adhesion, void content, and fracture causes. The instrument parameters comprised a resolution of 1.5 nm at an accelerating voltage of 30 kV, a working distance of 10 mm, and secondary electron imaging capabilities (Hi-Resolution Scanning Electron Microscope (HRSEM) Thermo Sceintific Apreo S, Waltham, MA, USA). The magnification was established at 5X, with a working distance of 48 mm or less, and the electron gun functioned within an accelerating voltage range of 0.5–30 kV. The HR-SEM images elucidated the failure mechanisms and the effects of GO integration on the composite architecture.

2.10 Thermogravimetric analysis (TGA)

TGA of the thermal degradation characteristics of CFRP composites with differing GO concentrations was carried out using a Jupiter STA 449 F3 thermal analyzer (NETZSCH, Germany) in a nitrogen environment to avoid oxidative damage. The samples were heated from 30 °C to 1000 °C at a constant rate of 10 °C/min. For each test, specimens weighing approximately 10 ± 1 mg were used. To ensure a consistent fiber-to-resin ratio across all samples, the test specimens were carefully cut from the central region of the composite laminates, where uniform fiber distribution and resin impregnation were ensured. This procedure minimizes variability and enables accurate comparison of thermal degradation and residual masses across different GO concentrations.

2.11 Differential scanning calorimetry (DSC)

DSC analysis of CFRP/epoxy composites containing various GO concentrations was carried out using the Jupiter STA 449 F3 thermal analyzer (NETZSCH, Germany). Each sample weighing 10 ± 1 mg was placed in an aluminum pan and heated from 30 °C to 1000 °C at a constant heating rate of 10 °C/min. The tests were conducted under a nitrogen atmosphere with a flow rate of 20 mL/min to prevent oxidation, ensure uniform heat transfer, and remove volatile components during heating. The obtained thermograms were used to determine the glass transition temperature (T_g) and other characteristic features of the composites.

3 Results and discussion

The outcomes of the tensile, flexural, impact, and flammability tests underscore the unique properties of the materials. The tensile test checks the material's strength under tensile stresses, the flexural test evaluates its resistance to bending, the impact test measures its capacity to endure abrupt shocks, and the flammability test quantifies its ability to resist fire.

3.1 HR-SEM morphology of CFRP composites

Fig. 7 presents the HR-SEM images of CFRP/epoxy and GO/CFRP/epoxy composites. Fig. 7 (a) illustrates the shape of the CFRP/epoxy composite devoid of GO. Fig. 7 (b) to (e) represents the distribution of GO within the epoxy matrix. Fig. 7 (b) demonstrates that the GO are uniformly distributed throughout the epoxy matrix, exhibiting negligible agglomeration. With an increase in GO content, there is a decrease in void formation and a more homogeneous distribution of GO, as illustrated in Fig. 7 (c) to (e). The enhanced dispersion of GO within the matrix reduces the occurrence of micro-voids and enhances the composite's overall structural integrity. This produces a more uniform material with potentially enhanced mechanical and thermal properties, demonstrating the beneficial impact of GO on the composite's performance.

3.2 XRD analysis

The XRD examination of CFRP composites with different GO concentrations (0, 0.05, 0.1, 0.3, and 0.5 wt.%) indicates substantial structural alterations. The prominent peak within the 2θ range 20–30° signifies the amorphous characteristics of the polymer matrix, whilst the heightened diffraction peak at around 25.28° with escalating

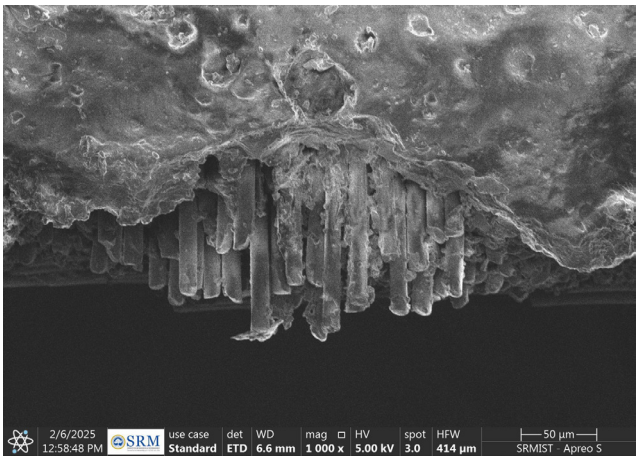

(a)

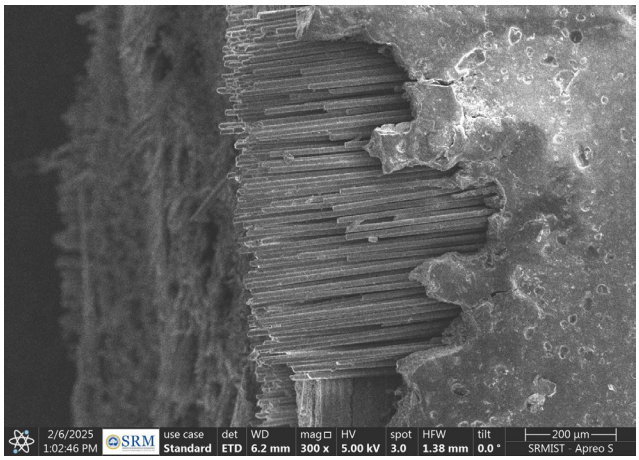

(b)

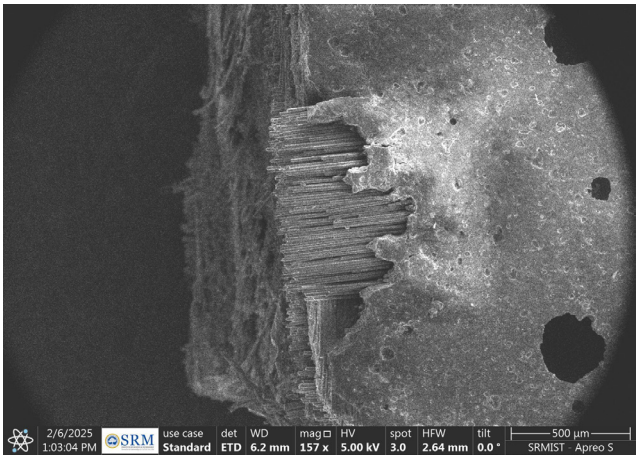

(c)

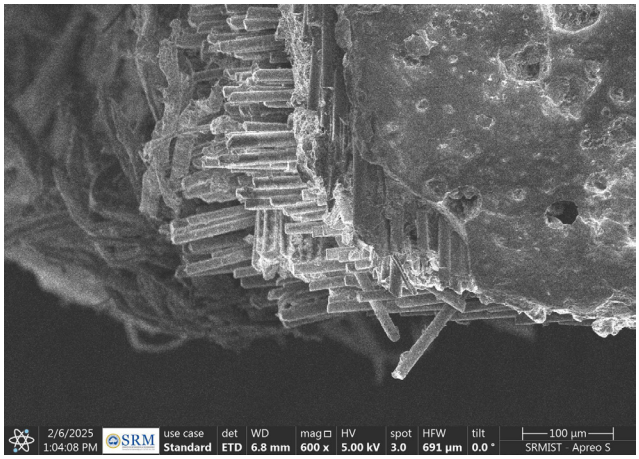

(d)

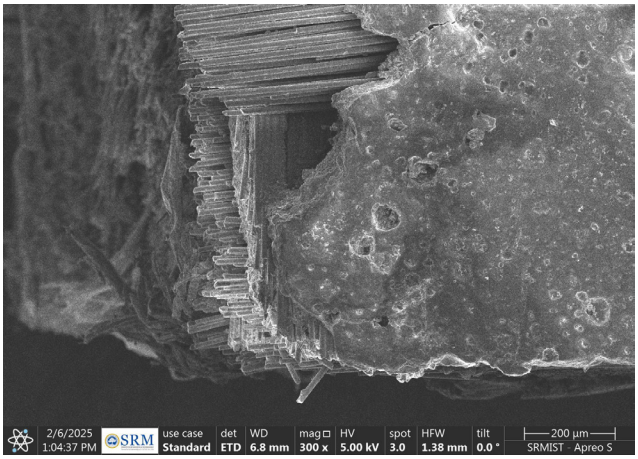

(e)

Fig. 7 (a) CFRP/epoxy composites; (b) 0.05 wt.% GO/CFRP/epoxy; (c) 0.1 wt.% GO/CFRP/epoxy; (d) 0.3 wt.% GO/CFRP/epoxy; (e) 0.5 wt.% GO/CFRP/epoxy

GO concentration suggests enhanced graphitic ordering. The highest peak was noted at 0.5 wt.% GO, indicating a higher degree of graphitic stacking. At 0.3 wt.% GO, a relatively sharp but moderate-intensity peak suggests better dispersion, leading to superior mechanical strength and thermal stability. At 0.5 wt.%, GO, peak broadening, and diminished intensity suggest potential GO aggregation, which could impede effective stress transfer and compromise structural integrity. The supplementary peaks at around 43.80° and 48.06° validate the structural enhancement of GO inclusion, as shown in Fig. 8. The results indicate that 0.3 wt.% GO achieves the optimal equilibrium

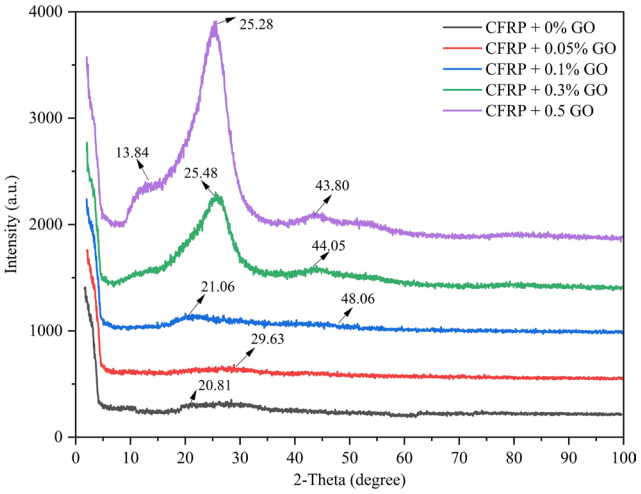

Fig. 8 XRD pattern for the CFRP composite

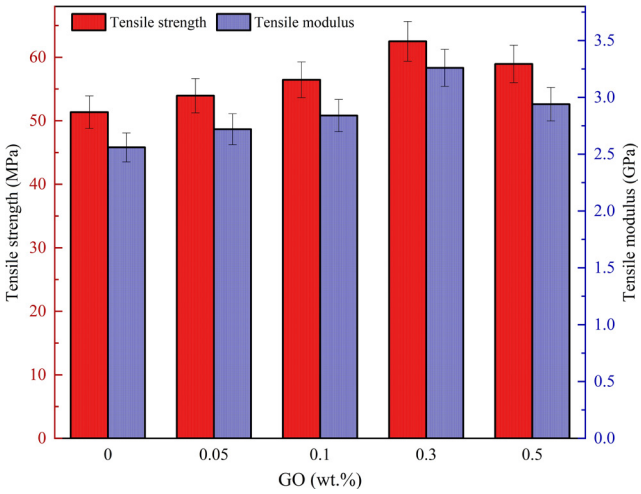

Fig. 9 Tensile strength and tensile modulus of CFRP composite

between dispersion and crystallinity, rendering it the ideal concentration for improving CFRP composite performance in structural applications.

3.3 Tensile test

In the tensile strength neat resin refers to the pure epoxy matrix without any fiber or GO reinforcement. It serves as a baseline for evaluating the mechanical improvement provided by CFRP and GO-enhanced composites. The average tensile strength and Young's modulus of the neat epoxy resin were recorded as 11.42 MPa and 1.37 GPa, respectively. The tensile strength and modulus of the CFRP composite were enhanced with the incorporation of GO, attaining maximum values at 0.3 wt.%. The tensile strength enhanced from 51.36 MPa (neat resin) to 62.51 MPa, indicating a 21.7% rise, and the tensile modulus increased from 2.56 GPa to 3.26 GPa, reflecting a 27.3% gain. This improvement is due to the superior mechanical characteristics of GO and its capacity to augment stress transmission inside the polymer matrix. At lower concentrations (0.05 wt.% and 0.1 wt.%), the GO exhibited effective dispersion, facilitating incremental enhancement and rigidity of the composite. At 0.5 wt.%, both tensile strength and modulus decreased to 58.95 MPa and 2.94 GPa, respectively, as shown in Fig. 9, due to GO agglomeration, which causes inadequate interfacial adhesion, unequal stress distribution, and defect formation. This suggests that surplus GO beyond a threshold concentration instead of dispersing uniformly, adversely impacting mechanical performance. Consequently, 0.3 wt.% is recognized as the optimal GO content, achieving a balance between enhanced mechanical characteristics and effective dispersion, thus being the most efficacious reinforcement level for augmenting the tensile performance of the composite. Table 2 summarizes the mechanical properties of CFRPs incorporated with functionalized GO nanoparticles.

3.4 Flexure test

The flexural strength and modulus of the CFRP composite were enhanced with the incorporation of GO, attaining peak values at 0.3 wt.%. The flexural strength rose from 96.54 MPa (neat resin) to 126.52 MPa, reflecting a 31.1% improvement, while the flexural modulus climbed from 3.56 GPa to 4.65 GPa, indicating a 30.6% enhancement. This enhancement is ascribed to the superior reinforcing properties of GO, which improves stress transfer and increases the rigidity of the polymer matrix. At lower GO concentrations (0.05 wt.% and 0.1 wt.%), both strength and modulus gradually enhanced owing to the homogeneous dispersion of GO, resulting in improved load distribution, as shown in Fig. 10. At 0.5 wt.%, the flexural strength and modulus decreased to 117.41 MPa and 4.37 GPa due to GO agglomeration, compromising interfacial adhesion and creating stress concentration spots. This aggregation restricts the efficient load transfer and induces flaws in the composite. Consequently, 0.3 wt.% is recognized as the ideal GO concentration, offering the optimal equilibrium of strength, stiffness, and dispersion, thereby serving as the most efficacious reinforcement level for improving the flexural performance of the composite.

3.5 Impact strength

The impact strength of the CFRP composite was enhanced with the incorporation of GO, attaining a peak value of 0.3 wt.%. The impact strength rose from 10.58 kJ/m^2 (neat resin/CFRP) to 14.63 kJ/m^2, indicating a 38.2% enhancement. This improvement is due to GO capacity to absorb

Table 2 Results of mechanical properties of CFRP composite

GO (wt.%)	Tensile strength (MPa) ± SD	Tensile modulus (GPa) ± SD	Flexural strength (MPa) ± SD	Flexural modulus (GPa) ± SD	Impact strength (kJ/m²) ± SD
GO-0	51.36 ± 1.54	2.56 ± 0.08	96.54 ± 2.90	3.56 ± 0.11	10.58 ± 0.42
GO-0.05	53.95 ± 1.62	2.72 ± 0.09	106.45 ± 3.19	2.74 ± 0.08	11.96 ± 0.48
GO-0.1	56.45 ± 1.69	2.84 ± 0.09	112.85 ± 3.38	4.12 ± 0.12	12.54 ± 0.50
GO-0.3	62.51 ± 1.88	3.26 ± 0.10	126.52 ± 3.80	4.65 ± 0.14	14.63 ± 0.58
GO-0.5	58.95 ± 1.77	2.94 ± 0.09	117.41 ± 3.52	4.37 ± 0.13	13.45 ± 0.54

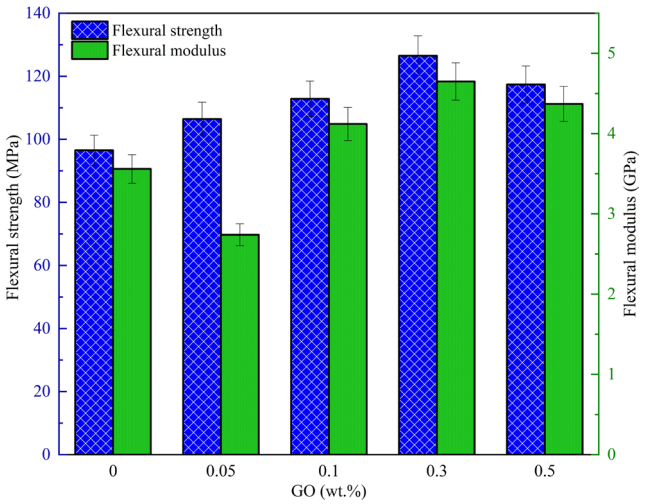

Fig. 10 Result of flexural strength

impact energy and augment crack resistance *via* mechanisms including crack deflection, energy dissipation, and enhanced interfacial interaction with the matrix. At lower concentrations (0.05 wt.% and 0.1 wt.%), the impact strength progressively increased due to uniform dispersion and improved energy absorption.

At 0.5 wt.%, the impact strength decreased to 13.45 kJ/m², presumably due to GO agglomeration, which induces localized stress concentrations and decreases the composite's overall toughness, as shown in Fig. 11. This indicates

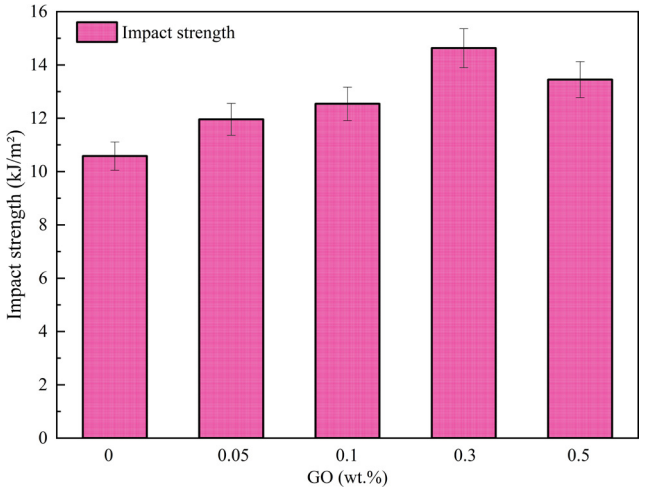

Fig. 11 Result of impact strength

that. In contrast, GO improves impact strength, excessive loading results in inadequate dispersion and adversely affects performance. Consequently, 0.3 wt.% is the ideal GO concentration for maximizing impact resistance while ensuring adequate dispersion within the polymer matrix.

Table 3 compares the mechanical properties of GO-reinforced CF/epoxy composites from the present study with those reported in the selected literature [27–36]. Among the referenced studies, Jenkins et al. [27] and Wang et al. [29] reported lower flexural strength values (62 MPa and 93.38 MPa), suggesting limited improvement at the same GO content. In contrast, Kumar and Verma [28] showed significantly higher flexural strength (170 MPa), possibly due to differences in GO type, dispersion method, or composite fabrication. Meanwhile, Pramodkumar and Budhe [30] used a higher GO loading (1.5 wt.%) and achieved only moderate flexural strength (80.2 MPa), whereas Arun et al. [31] with 2.5 wt.% GO observed a substantial reduction in both tensile and flexural strength, likely due to filler agglomeration.

3.6 Water absorption test

Water absorption in CFRP/epoxy composites is influenced by the fiber–matrix interface and GO content. Due to CFRP's hydrophobic nature, the unmodified composite (GO-0) exhibited a water uptake of 0.14%. With the addition of GO, water absorption gradually decreased to 0.05% at 0.5 wt.% GO, as presented in Table 4. This reduction is attributed to the barrier effect of GO, which restricts epoxy chain mobility and increases the tortuosity of water diffusion paths, thereby enhancing the composite's resistance to moisture ingress.

3.7 Flammability tests

3.7.1 Horizontal flame test

Table 5 presents the horizontal flame test findings on CFRP/epoxy composites infused with GO, indicating a distinct enhancement in flame-retardant qualities with increasing GO content. The duration of flame propagation

Table 3 Comparison of mechanical properties of GO-reinforced CF/epoxy composites from literature and this study

Composite	Matrix	Fillers	Filler content (%)	Tensile strength (MPa)	Tensile modulus (GPa)	Flexural strength (MPa)	Flexural modulus (GPa)	Impact strength (kJ/m^2)	Reference
CF/GO/epoxy	Epoxy	GO	0.3	62.51	3.26	126.52	4.65	14.63	This study
CF/rGO/epoxy	Epoxy (IN2)	rGO	0.3	–	–	62	4.4	–	[27]
CF/rGO/epoxy	Epoxy	GO	0.3	88	–	170	4.46	–	[28]
CF/GO/PP	Polypropylene (PP)	GO	0.3	71.28	–	93.38	–	5.47	[29]
CF/GO/epoxy	Epoxy	GO	1.5	–	–	80.2	3.94	–	[30]
CF/GO/epoxy	Epoxy	GO	2.5	40.7	–	24.52	–	–	[31]
CF/GNPs/epoxy	Epoxy	GNP	0.3	76.9	–	–	–	–	[32]
CF/GO/epoxy	Epoxy	GO	0.4	55.4	2.6	–	–	–	[33]
CF/CNT/epoxy	Epoxy	CNT	0.3	81.7	2.8	–	–	–	[34]
CF/CF/epoxy	Epoxy	Ceramic particle	10	–	–	–	–	2.45	[35]
CF/GO/epoxy	Epoxy	GO	0.3	38.41	2.22	–	–	–	[36]

Table 4 Water absorption in CFRP composite samples

GO (wt.%)	Mass of sample before immersion (g)	Mass of sample after immersion (g)	Percentage of mass gain (%)
GO-0	8.856	8.868	0.14
GO-0.05	8.998	9.008	0.11
GO-0.1	9.052	9.059	0.08
GO-0.3	8.993	8.998	0.06
GO-0.5	8.851	8.855	0.05

Table 5 Results of the horizontal flame test

GO (wt.%)	Time of flame travel (s)	Flame travel (mm)	Burning rate (mm/min)
GO-0	259	103	23.86
GO-0.05	265	95	21.51
GO-0.1	234	79	20.26
GO-0.3	198	63	19.09
GO-0.5	176	54	18.41

diminishes with elevated GO concentration, decreasing from 259 sec at 0 wt.% to 176 sec at 0.5 wt.%, signifying a more rapid flame spread in the empty composite and deceleration as GO content increases. Correspondingly, the flame travel distance diminishes from 103 mm at 0 wt.% to 54 mm at 0.5 wt.%, further highlighting the inhibitory influence of GO on flame propagation. The burning rate, defined as the flame propagation distance per min, diminishes from 23.86 mm/min at 0 wt.% to 18.41 mm/min at 0.5 wt.%. The decrease in the burning rate underscores GO significant contribution to improving the fire resistance of CFRP/epoxy composites, presumably attributable to its flame-retardant characteristics that inhibit flame propagation and facilitate flame extinguishment.

3.7.2 Vertical flame test

The vertical flame test results for CFRP composites containing GO are displayed in Table 6. The flame resistance of the

Table 6 Results of the vertical flame test

GO (wt.%)	Self-extinguishing time (s)	Cotton ignited by flaming drips	Rating
GO-0	34	NO	V-1
GO-0.05	27	NO	V-1
GO-0.1	21	NO	V-1
GO-0.3	14	NO	V-1
GO-0.5	8	NO	V-0

composite materials was assessed by measuring self-extinguishing time and the occurrence of flaming drops. All specimens were evaluated for their capacity to self-extinguish upon exposure to flame, revealing a reduction in self-extinguishing time correlated with greater GO concentration. The control sample (0 wt.%) demonstrated a self-extinguishing time of 34 s and received a V-1 rating, signifying moderate flame resistance without flaming droplets. Comparable ratings were noted for the GO-filled CFRP composites at 0.05 wt.% and 0.1 wt.% GO, exhibiting self-extinguishing periods of 27 s and 21 s, respectively. The samples showed no flaming drips and received a V-1 rating.

This indicates that incorporating low amounts of GO into the CFRP matrix enhances flame resistance, albeit the performance remains within the V-1 classification. At 0.3 wt.% GO, the self-extinguishing duration further diminished to 14 s, and the sample exhibited no burning drips, preserving the V-1 grade. The self-extinguishing time diminished with increasing GO concentration, with the 0.5 wt.% sample demonstrating a very rapid self-extinguishing time of under 8 s, without any burning droplets seen. This sample received a V-0 rating, signifying the utmost degree of flame resistance as per vertical flame test criteria. The enhancement of flame resistance with elevated GO content is due to the development of a robust, stable char layer during combustion. GO, functioning as a flame-retardant agent, facilitates the formation of a char layer that acts as a thermal barrier and restricts the emission of flammable volatiles from the epoxy resin matrix. The improved flame retardancy noted in the 0.5 wt.% GO sample, classified as V-0, aligns with results from analogous composite investigations, which demonstrate that GO enhances flame resistance by preventing the generation of flame drips and diminishing the overall combustibility of the matrix.

3.8 FTIR analysis

Fig. 12 displays the FTIR spectra of CFRP composites with varying GO concentrations (0%, 0.05%, 0.1%, 0.3%, and 0.5%) in the wavenumber range of 4000–500 1/cm. The broad absorption band observed between 3600 and 3747 1/cm corresponds to O−H stretching vibrations, signifying the presence of hydroxyl groups originating from the epoxy resin and residual functional groups in GO. The 2927 1/cm and 2366 1/cm peaks correspond to C−H stretching vibrations, indicative of aliphatic chains in the epoxy polymer. A prominent signal at approximately 1746 1/cm is attributed to C=O stretching vibrations, confirming the presence of ester and carbonyl

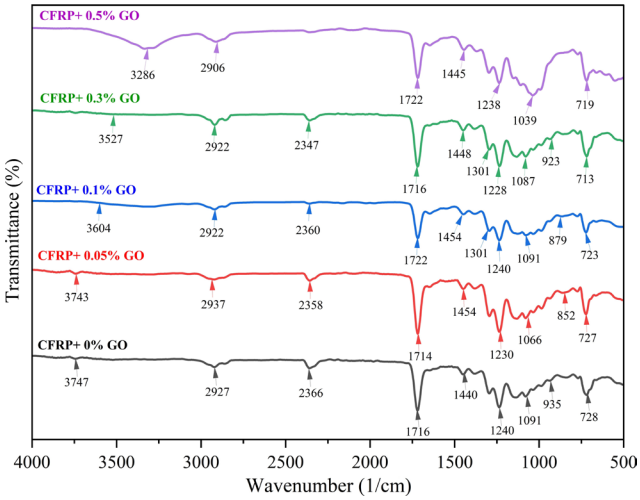

Fig. 12 FTIR analysis for the CFRP composite

functional groups, which may result from the oxidation of epoxy or residual oxygen-containing groups in GO [37]. The C−O−C stretching vibrations of epoxy ether linkages are in the 1240–1260 1/cm range. Furthermore, 1050–1150 1/cm range peaks indicate C−O stretching, reinforcing the interaction between epoxy and GO. An increase in GO concentration significantly alters peak locations and intensity, indicating robust interfacial interactions between GO and the epoxy matrix. The peaks between 800 and 900 1/cm correspond to the skeletal vibrations of GO, affirming the effective dispersion of GO within the CFRP composite. The spectral fluctuations indicate a sufficient chemical interaction between the epoxy matrix and GO, resulting in enhanced interfacial adhesion and potential improvements in mechanical properties.

3.9 TGA

Fig. 13 displays the TGA curves of CFRP composites with 0, 0.05, 0.1, 0.3, and 0.5 wt.% GO. All samples demonstrate a characteristic two-step deterioration pattern. The initial mass loss observed below approximately 100 °C is attributed to the evaporation of physically adsorbed moisture. Significant thermal degradation commences at approximately 300 °C and persists until 600 °C, primarily due to the disintegration of the polymer matrix, including epoxy resin and related constituents. Among all samples, CFRP with 0.5 wt.% GO exhibits the most excellent thermal stability, with a residual mass of roughly 69% at 800 °C, in contrast to 60% for the unmodified CFRP (0 wt.% GO). This improvement is due to the superior barrier characteristics of GO, which impede thermal diffusion and degradation. GO likely facilitates char formation and enhances the composite's resilience to thermal degradation. The significant mass

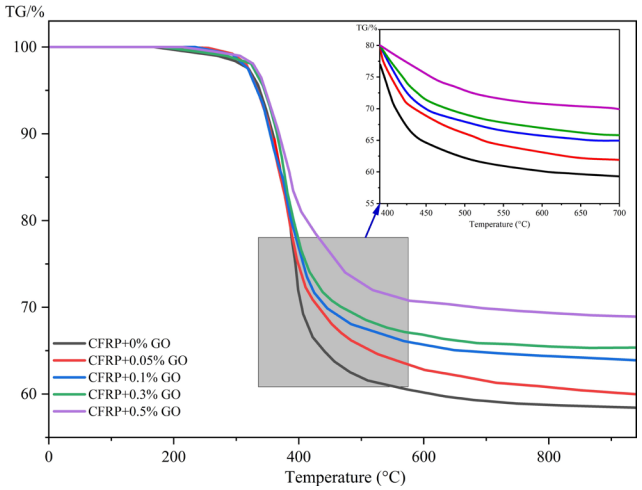

Fig. 13 Typical TGA curves of the different CFRP laminated composites

loss at 350–400 °C indicates the primary decomposition of the matrix resin. The alteration in degradation initiation temperatures and the augmented residue with elevated GO content further substantiate the beneficial effect of GO in improving the thermal stability of the composites.

3.10 DSC analysis

DSC was employed to determine the T_g of the CFRP/epoxy composites. As shown in Fig. 14, T_g was identified from the inflection point of the baseline shift in the DSC thermograms, occurring between approximately 102–173 °C, which is consistent with typical DGEBA-based epoxy systems. The neat CFRP laminate exhibited a T_g of 102.31 °C, which increased to 132.40 °C, 143.10 °C, 163.16 °C, and 169.18 °C for composites containing 0.05, 0.1, 0.3, and 0.5 wt.% GO, respectively. This progressive increase in T_g indicates that GO incorporation effectively restricts polymer chain mobility through enhanced interfacial bonding and increased crosslink density within the epoxy matrix. In addition to T_g, minor deviations and peaks beyond the transition region were observed, which are attributed to secondary relaxation processes or residual curing reactions, while higher-temperature endothermic features are associated with thermal decomposition of the epoxy matrix, consistent with the Tonset and Tmax values confirmed by TGA analysis. As a result, the composites demonstrate improved dimensional stability and mechanical performance at elevated service temperatures, which is advantageous for structural applications requiring enhanced thermal resistance.

4 Conclusion

This study demonstrated that the incorporation of GO into CFRP/epoxy composites significantly enhanced their mechanical, thermal, and flame-retardant properties. Among the tested concentrations, 0.3 wt.% GO was found to be optimal. At this level, the composite exhibited a 21.7% increase in tensile strength, 27.3% increase in tensile modulus, 31.1% improvement in flexural strength, and 38.2% enhancement in impact strength compared to the neat CFRP composite. These improvements are primarily attributed to the high surface area and mechanical integrity of GO, which facilitate effective stress transfer and microstructural reinforcement within the polymer matrix. Thermal analysis revealed increased thermal stability and a higher T_g with GO

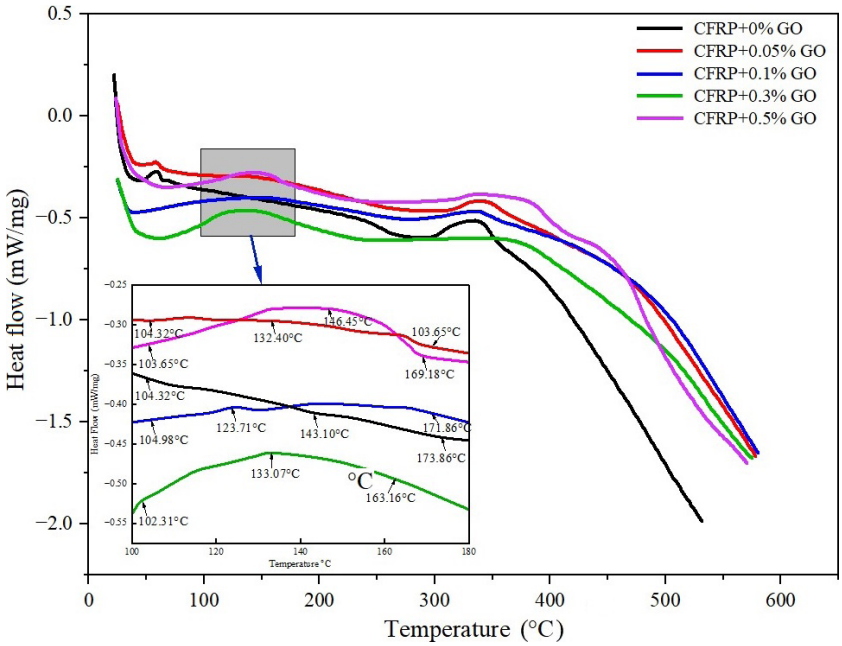

Fig. 14 DSC curves of the different CFRP laminated composites

incorporation. Additionally, the flame-retardant behavior improved significantly, with the 0.5 wt.% GO/CFRP composite achieving a V-0 rating in the horizontal burning test. However, excessive filler loading beyond 0.3 wt.% resulted in agglomeration, leading to reduced performance due to weak interfacial bonding and stress concentration. Overall, 0.3 wt.% GO was identified as the most effective concentration for balancing strength, thermal resistance, and flame retardancy. Future research should explore environmental durability, long-term aging, and performance under elevated temperatures to ensure suitability for advanced structural and fire-critical applications.

References

[1] Harle, S. M. "Durability and long-term performance of fiber reinforced polymer (FRP) composites: A review", Structures, 60, 105881, 2024. https://doi.org/10.1016/j.istruc.2024.105881

[2] Vijayan, D. S., Sivasuriyan, A., Devarajan, P., Stefańska, A., Wodzyński, Ł., Koda, E. "Carbon Fibre-Reinforced Polymer (CFRP) Composites in Civil Engineering Application—A Comprehensive Review", Buildings, 13(6), 1509, 2023. https://doi.org/10.3390/buildings13061509

[3] Saeed, F. H., Hejazi, F., Rashid, R. S. M. "Strengthening of reinforced concrete slabs using carbon fiber reinforced polymers rods and concrete jacket with a mechanical anchorage system", Construction and Building Materials, 440, 137464, 2024. https://doi.org/10.1016/j.conbuildmat.2024.137464

[4] Zhou, S. C., Demartino, C., Xu, J. J., Xiao, Y. "Effectiveness of CFRP seismic-retrofit of circular RC bridge piers under vehicular lateral impact loading", Engineering Structures, 243, 112602, 2021. https://doi.org/10.1016/j.engstruct.2021.112602

[5] Alsuhaibani, E. "Optimization of Carbon Fiber-Reinforced Polymer (CFRP) Configuration for Enhanced Flexural Performance in Strengthened Concrete Beams", Buildings, 14(12), 3953, 2024. https://doi.org/10.3390/buildings14123953

[6] Qi, X., Tian, J., Xian, G. "Hydrothermal ageing of carbon fiber reinforced polymer composites applied for construction: A review", Journal of Materials Research and Technology, 27, pp. 1017–1045, 2023. https://doi.org/10.1016/j.jmrt.2023.09.198

[7] Wei, H., Xia, J., Zhou, W., Zhou, L., Hussain, G., Li, Q., Ostrikov, K. K. "Adhesion and cohesion of epoxy-based industrial composite coatings", Composites Part B: Engineering, 193, 108035, 2020. https://doi.org/10.1016/j.compositesb.2020.108035

[8] Galińska, A. "Mechanical Joining of Fibre Reinforced Polymer Composites to Metals—A Review. Part I: Bolted Joining", Polymers, 12(10), 2252, 2020. https://doi.org/10.3390/polym12102252

[9] Bisht, N., Vishwakarma, J., Jaiswal, S., Kumar, P., Srivastava, A. K., Dhand, C., Dwivedi, N. "Synergizing chemistry: unveiling the potential of hybrid fillers for enhanced performance in shape memory polymers", Advanced Composites and Hybrid Materials, 8(1), 7, 2024. https://doi.org/10.1007/s42114-024-01059-2

[10] Sayam, A., Rahman, A. N. M. M., Rahman, M. S., Smriti, S. A., Ahmed, F., Rabbi, M. F., Hossain, M., Faruque, M. O. "A review on carbon fiber-reinforced hierarchical composites: mechanical performance, manufacturing process, structural applications and allied challenges", Carbon Letters, 32(5), pp. 1173–1205, 2022. https://doi.org/10.1007/s42823-022-00358-2

[11] Mohan, V. B., Lau, K., Hui, D., Bhattacharyya, D. "Graphene-based materials and their composites: A review on production, applications and product limitations", Composites Part B: Engineering, 142, pp. 200–220, 2018. https://doi.org/10.1016/j.compositesb.2018.01.013

[12] Zhao, Y., Lin, W., Edwards, G., Zou, Y., Zhao, X., Song, S., Heitzmann, M., Martin, D., Grøndahl, L., Lu, M., Huang, H. "Graphene/graphene oxide and melamine as synergistic additives for polyester nanocomposite coatings", Materials Chemistry and Physics, 320, 129384, 2024. https://doi.org/10.1016/j.matchemphys.2024.129384

[13] Li, M., Deng, T., Zheng, B., Zhang, Y., Liao, Y., Zhou, H. "Effect of Defects on the Mechanical and Thermal Properties of Graphene", Nanomaterials, 9(3), 347, 2019. https://doi.org/10.3390/nano9030347

[14] Hung, P., Lau, K., Fox, B., Hameed, N., Lee, J. H., Hui, D. "Surface modification of carbon fibre using graphene–related materials for multifunctional composites", Composites Part B: Engineering, 133, pp. 240–257, 2018. https://doi.org/10.1016/j.compositesb.2017.09.010

[15] Selim, M. S., El-Safty, S. A., Shenashen, M. A., Elmarakbi, A. "Advances in polymer/inorganic nanocomposite fabrics for lightweight and high-strength armor and ballistic-proof materials", Chemical Engineering Journal, 493, 152422, 2024. https://doi.org/10.1016/j.cej.2024.152422

[16] Gupta, R., Singh, M. K., Rangappa, S. M., Siengchin, S., Dhakal, H. N., Zafar, S. "Recent progress in additive inorganic flame retardants polymer composites: Degradation mechanisms, modeling and applications", Heliyon, 10(21), e39662, 2024. https://doi.org/10.1016/j.heliyon.2024.e39662

[17] Parvizi, P., Jalilian, M., Dearn, K. D. "Epoxy composites reinforced with nanomaterials and fibres: Manufacturing, properties, and applications", Polymer Testing, 146, 108761, 2025. https://doi.org/10.1016/j.polymertesting.2025.108761

[18] Motta de Castro, E., Bozorgmehrian, F., Carrola, M., Koerner, H., Samouei, H., Asadi, A. "Sulfur-driven reactive processing of multiscale graphene/carbon fiber- polyether ether ketone (PEEK) composites with tailored crystallinity and enhanced mechanical performance", Composites Part B: Engineering, 295, 112180, 2025. https://doi.org/10.1016/j.compositesb.2025.112180

[19] Wagh, S. S., Shelake, H. D., Chougale, A. S., Topare, N. S., Gunnasegaran, P., Syed, A. !Nanoparticles and Nanofillers: A Promising Future Drug Delivery Industry", In: Mallakpour, S., Hussain, C. M. (eds.) Handbook of Nanofillers, pp. 1–28. ISBN 978-981-99-3516-1 https://doi.org/10.1007/978-981-99-3516-1_84-1

[20] Said, Z., Pandey, A. K., Tiwari, A. K., Kalidasan, B., Jamil, F., Thakur, A. K., Tyagi, V. V., Sarı, A., Ali, H. M. "Nano-enhanced phase change materials: Fundamentals and applications", Progress in Energy and Combustion Science, 104, 101162, 2024. https://doi.org/10.1016/j.pecs.2024.101162

[21] Mishra, T., Mandal, P., Rout, A. K., Sahoo, D. "A state-of-the-art review on potential applications of natural fiber-reinforced polymer composite filled with inorganic nanoparticle", Composites Part C: Open Access, 9, 100298, 2022. https://doi.org/10.1016/j.jcomc.2022.100298

[22] Ramesh, M., Rajeshkumar, L. N., Srinivasan, N., Kumar, D. V., Balaji, D. "Influence of filler material on properties of fiber-reinforced polymer composites: A review", e-Polymers, 22(1), pp. 898–916, 2022. https://doi.org/10.1515/epoly-2022-0080

[23] ASTM International "ASTM D638-14 Standard Test Method for Tensile Properties of Plastics", ASTM International, West Conshohocken, PA, USA, 2015. https://doi.org/10.1520/D0638-14

[24] ASTM International "ASTM D790-17 Standard Test Methods for Flexural Properties of Unreinforced and Reinforced Plastics and Electrical Insulating Materials", ASTM International, West Conshohocken, PA, USA, 2017. https://doi.org/10.1520/D0790-17

[25] ASTM International "ASTM D256-24 Standard Test Methods for Determining the Izod Pendulum Impact Resistance of Plastics", ASTM International, West Conshohocken, PA, USA, 2024. https://doi.org/10.1520/D0256-24

[26] ASTM International "ASTM D570-22 Standard Test Method for Water Absorption of Plastics", ASTM International, West Conshohocken, PA, USA, 2022. https://doi.org/10.1520/D0570-22

[27] Jenkins, P., Siddique, S., Khan, S., Usman, A., Starost, K., MacPherson, A., Bari, P., Mishra, S., Njuguna, J. "Influence of Reduced Graphene Oxide on Epoxy/Carbon Fiber-Reinforced Hybrid Composite: Flexural and Shear Properties under Varying Temperature Conditions", Advanced Engineering Materials, 21(6), 1800614, 2019. https://doi.org/10.1002/adem.201800614

[28] Kumar, J., Verma, R. K. "Experimental investigation for machinability aspects of graphene oxide/carbon fiber reinforced polymer nanocomposites and predictive modeling using hybrid approach", Defence Technology, 17(5), pp. 1671–1686, 2021. https://doi.org/10.1016/j.dt.2020.09.009

[29] Wang, C.-C., Zhao, Y.-Y., Ge, H.-Y., Qian, R.-S. "Enhanced mechanical and thermal properties of short carbon fiber reinforced polypropylene composites by graphene oxide", Polymer Composites, 39(2), pp. 405–413, 2018. https://doi.org/10.1002/pc.23950

[30] Pramodkumar, B., Budhe, S. "The effect of graphene oxide on thermal, electrical, and mechanical properties of carbon/epoxy composites: Towards multifunctional composite material", Polymer Composites, 45(7), pp. 6374–6384, 2024. https://doi.org/10.1002/pc.28203

[31] Arun, G. K., Sreenivas, N., Reddy, K. B., Krishna Reddy, K. S., Shashi Kumar, M. E., Pramod, R. "Investigation on Mechanical Properties of Graphene Oxide reinforced GFRP", IOP Conference Series: Materials Science and Engineering, 310(1), 012158, 2018. https://doi.org/10.1088/1757-899X/310/1/012158

[32] Topkaya, T., Çelik, Y. H., Kilickap, E. "Mechanical properties of fiber/graphene epoxy hybrid composites", Journal of Mechancial Science and Technology, 34(11), pp. 4589–4595, 2020. https://doi.org/10.1007/s12206-020-1016-4

[33] Mirzapour, M., Cousin, P., Robert, M., Benmokrane, B. "Dispersion Characteristics, the Mechanical, Thermal Stability, and Durability Properties of Epoxy Nanocomposites Reinforced with Carbon Nanotubes, Graphene, or Graphene Oxide", Polymers, 16(13), 1836, 2024. https://doi.org/10.3390/polym16131836

[34] Prasanthi, P. P., Kumar, M. S. R. N., Chowdary, M. S., Madhav, V. V. V., Saxena, K. K., Mohammed, K. A., Khan, M. I., Upadhyay, G., Eldin, S. M. "Mechanical properties of carbon fiber reinforced with carbon nanotubes and graphene filled epoxy composites: experimental and numerical investigations", Materials Research Express, 10(2), 025308, 2023. https://doi.org/10.1088/2053-1591/acaef5

[35] Ali, N. H., Shihab, S. K., Mohamed, M. T. "Influence of Ceramic Particles Additives on the Mechanical Properties and Machinability of Carbon Fiber/Polymer Composites", Silicon, 15(13), pp. 5485–5502, 2023. https://doi.org/10.1007/s12633-023-02449-9

[36] Xu, T., Zhou, S., Cui, S., Song, N., Shi, L., Ding, P. "Three-dimensional carbon fiber-graphene network for improved thermal conductive properties of polyamide-imide composites", Compos Part B: Engineering, 178, 107495, 2019. https://doi.org/10.1016/j.compositesb.2019.107495

[37] Bellussi, F. M., Sáenz Ezquerro, C., Laspalas, M., Chiminelli, A. "Effects of Graphene Oxidation on Interaction Energy and Interfacial Thermal Conductivity of Polymer Nanocomposite: A Molecular Dynamics Approach", Nanomaterials, 11(7), 1709, 2021. https://doi.org/10.3390/nano11071709